Results in Physics 6 (2016) 299–304

Contents lists available at ScienceDirect

Results in Physics

journal homepage: www.journals.elsevier.com/results-in-physics

Preparation and antibacterial activities of $Ag/Ag^{+}/Ag^{3+}$ nanoparticle composites made by pomegranate (*Punica granatum*) rind extract

Yang Hui [a,*], Ren Yan-yu [a], Wang Tao [a], Wang Chuang [b]

[a] School of Food & Biological Engineering, Shaanxi University of Science & Technology, Xi'an 710021, PR China
[b] Department of Highway & Bridge, Shaanxi Railway Institute, Weinan 714000, PR China

ARTICLE INFO

Article history:
Received 9 May 2016
Accepted 31 May 2016
Available online 3 June 2016

Keywords:
Pomegranate rind
Biosynthesis
$Ag/Ag^{+}/Ag^{3+}$ nanoparticle composites
Antibacterial activity

ABSTRACT

Nano-silver and its composite materials are widely used in medicine, food and other industries due to their strong conductivity, size effect and other special performances. So far, more microbial researches have been applied, but a plant method is rarely reported. In order to open up a new way to prepare AgNP composites, pomegranate peel extract was used in this work to reduce Ag^{+} to prepare $Ag/Ag^{+}/Ag^{3+}$ nanoparticle composites. UV–Vis was employed to detect and track the reduction of Ag^{+} and the forming process of AgNPs. The composition, structure and size of the crystal were analyzed by XRD and TEM. Results showed that, under mild conditions, pomegranate peel extract reacted with dilute $AgNO_3$ solution to produce $Ag/Ag^{+}/Ag^{3+}$ nanoparticle composites. At pH = 8 and 10 mmol/L of $AgNO_3$ concentration, the size of the achieved composites ranged between 15 and 35 nm with spherical shapes and good crystallinity. The bactericidal experiment indicated that the prepared $Ag/Ag^{+}/Ag^{3+}$ nanoparticles had strong antibacterial activity against gram positive bacteria and gram negative bacteria. FTIR analysis revealed that biological macromolecules with groups of $—NH_2$, —OH, and others were distributed on the surface of the newly synthesized $Ag/Ag^{+}/Ag^{3+}$ nanoparticles. This provided a useful clue to further study the AgNP biosynthesis mechanism.

Introduction

Ag nanoparticles (AgNPs) have unique physical and chemical properties, hence widely used in many fields. Their huge specific surface area and high surface activity make them exhibit superior adsorption and become an excellent catalyst in heterogeneous catalytic reactions [1–3]. Their antibacterial ability is far greater than that of the traditional silver ion sterilization agents. So they have been widely used in household textiles, chemical building materials and medical and health fields [4–7]. Their good size effect and surface effect make them excellent electronic paste materials in electronics industry [8]. They are also used in the preparation of electrodes, biosensor, heat exchanger, and surface enhanced Raman scattering owing to their excellent thermal and electrical properties [9–11]. Therefore, it is of significance to study the preparation of silver nanoparticle composites.

Ag nanoparticles can be prepared by physical method, chemical method [12,13], photocatalysis, and biological method [14]. Compared to physical and chemical methods, the biological method is efficient, fast, stable, simple, eco-friendly, non-toxic, low-cost, and has many other advantages. So, it attracts more and more attention from the research circles [15]. The biosynthesis method includes syntheses by plants [16,17], animals and microorganisms [18,19]. There are abundant microbial species that are widely distributed in nature. The synthetic process is relatively simple and easy to operate. Therefore, the microbial synthesis of AgNPs has great potential, about which there are lots of reports [20].

Rajesh et al. [21] used the culture solution of *Lactobacillus acidophilus* to prepare AgNPs, in the process of which enzyme secreted in the culture solution by microorganisms played a key role in the reduction. Kiran et al. [22] used the culture solution of *Bacillus subtilis bacillus* to make AgNPs, in the process of which sugar ester surface active agents secreted in the culture solution of microorganism dispersed and protected AgNPs. Girilal et al. [23] used *thermophilic bacillus* extraction solution to achieve AgNPs. Parikh et al. [24] used silver nitrate to induce *morganella* secretion reducing substances to obtain AgNPs outside the cell, whereas Soni et al. [25] adopted nitrate silver to induce soil *fungi and Verticillium lecanii* to get AgNPs inside the cell.

Similar to microorganisms, animal and plant can produce reductase and reducing substances in the metabolic process. Both of them can be used to bio-synthesize Ag nanoparticles. In contrast,

* Corresponding author.

http://dx.doi.org/10.1016/j.rinp.2016.05.012
2211-3797/

the bio-synthesis of AgNPs using plants and animals as resources is rarely reported. In this aspect, the synthesis mechanism is under way.

Pomegranate peel extract contains polyphenols, amide and other reducing substances as well as amino acids, polysaccharides and other biological macromolecules. Therefore, in the present work, taking into account the principle of microbial biosynthesis of AgNPs, pomegranate peel extract was adopted to prepare $Ag/Ag^{+}/Ag^{3+}$ nanoparticle composites. The UV–Vis detection was applied to track the reduction of silver ions and the formation process of AgNPs. The structure, composition, surface morphology and antibacterial properties of the obtained composites were characterized. With the help of FTIR, the reason why the nanoparticles existed stably in the synthesis of $Ag/Ag^{+}/Ag^{3+}$ was analyzed, which laid a foundation for the further study of the preparation mechanism of AgNPs by plant extracts.

Materials and methods

Preparation of granatum extract

Fresh pomegranate skin was taken to be cleaned with deionized water for 3–5 times. 15 g of cleaned pomegranate peel was weighed and put into a 500 mL Erlenmeyer flask containing 200 mL of ultra pure water. The flask was placed in a water bath for 30 min with the temperature of 85 °C to efficiently get granatum extract, and then the obtained raw extract was filtered, and cooled. The achieved extract was used as a reducing agent and dispersant to prepare $Ag/Ag^{+}/Ag^{3+}$ nanocomposites.

Preparation of $Ag/Ag^{+}/Ag^{3+}$ nanoparticles

50 mL of pomegranate peel extract mixed with 100 mL of $AgNO_3$ solution (5 mmol/L, AR, Tianjin Kermel Chemical Reagent Co., Ltd) at room temperature. The mixture was magnetically stirred for 20 min and then placed in a water bath with the temperature of 35 °C. It was observed that the solution color turned slowly from light yellow to dark brown. The whole reduction reaction lasted for 1 h. The achieved colloid solution was denoted as S_1. Two samples of 50 mL of pomegranate bark extract were taken to mix with 100 mL of $AgNO_3$ solution at room temperature, respectively. 0.1 mmol/L ammonia solution was used to adjust two copies of pH of the mixed solution to 6 and 8, respectively, magnetically stirring for 10 min, and then the mixture was placed in a water bath of the temperature of 35 °C.

It was found that within 30 min the color of the solution of two copies of samples changed from light yellow to dark brown. The achieved two copies of colloid solutions were recorded as S_2 and S_3, respectively. After observation for three months, no color changes occurred in the colloidal solutions of S_2, S_3 and S_1 and no precipitation generated. The three copies of colloidal solutions were centrifuged at high speed for 10 min. The achieved precipitation was washed with 95% ethanol solution and ultra pure water, respectively, and then dried at 150 °C for 8 h. Thus, the $Ag/Ag^{+}/Ag^{3+}$ nanopowder composite was obtained.

Characterization of $Ag/Ag^{+}/Ag^{3+}$ nanocomposites

The colloidal solution was detected and tracked by UV visible spectrophotometer (UV–Vis, Unico Instrument, Shang-hai) to analyze the reduction of silver ion and the synthesis of AgNPs. The $Ag/Ag^{+}/Ag^{3+}$ nanocomposite powder was analyzed by X-ray diffraction (XRD, D/max-2200PC, Rigaku) to show the crystal composition and structure. The morphology and size was observed by transmission electron microscopy (TEM FEI, G2 F20 S-Twin, America). The infrared spectroscopy (FT-IR, VECTOR-22, Bruker Corporation of Germany) was applied to reveal the combination and distribution of biological macromolecules on the surface of the nanoparticles and to verify the stability and dispersion of the nanoparticles in the process of synthesis.

Antibacterial performance testing of $Ag/Ag^{+}/Ag^{3+}$ nanocomposites

The prepared $Ag/Ag^{+/}Ag^{3+}$ nanocomposites were tested by the inhibition zone method, respectively, against the antimicrobial resistances of gram negative *Escherichia coli* (*E. coli*) and gram positive *Staphylococcus aureus* (*S. aureus*). Each of two copies of 10 μL of *E. coli* and *S. aureus* after activated culture were taken, respectively, by a pipette to dilute 10 times. Then each of two copies of 50 μL solutions was taken to inject into itself LB nutrient agar medium plate. An applicator was used to smear it evenly. Then the 5 mm circular sterile filter papers, marked as Nos. 1–5 were placed on the surface of the agar medium plate. The No. 1 filter paper was denoted as the blank contrast sample; Nos. 2 and 4 filter papers contained, respectively, 10 μL of 1.16×10^{-4} mol/L and 7.23×10^{-6} mol/L $Ag/Ag^{+}/Ag^{3+}$ nanocomposites; Nos. 3 and 5 contained, respectively, 10 μL of the same concentration of AgNPs. The two experimental plats were placed in an incubator of 37 °C for culture for 24 h. The diameter (mm) of the inhibition zone was measured, which was regarded as a criterion to evaluate the antibacterial activity of the $Ag/Ag^{+}/Ag^{3+}$ nanocomposites.

Results and discussion

Analysis by UV–Vis and TEM

As shown in Fig. 1b, the color change in the colloidal solutions S_1, S_2 and S_3 was caused by the plasmon resonance (SPR) on the surface of the synthesized AgNPs in the reaction medium [26]. The tiny Ag particles appeared black, and the surface Ag^{+} was reduced to Ag. As shown in Fig. 1a, with the increase in the concentration of $AgNO_3$, the UV–Vis absorption peak gradually narrowed. When pH = 8 of the mixture solution and the concentration of $AgNO_3$ was 10 mmol/L, a sharp absorption peak appeared at 450 nm, suggesting that the grain size of the achieved AgNPs by reduction was smaller and distributed uniformly.

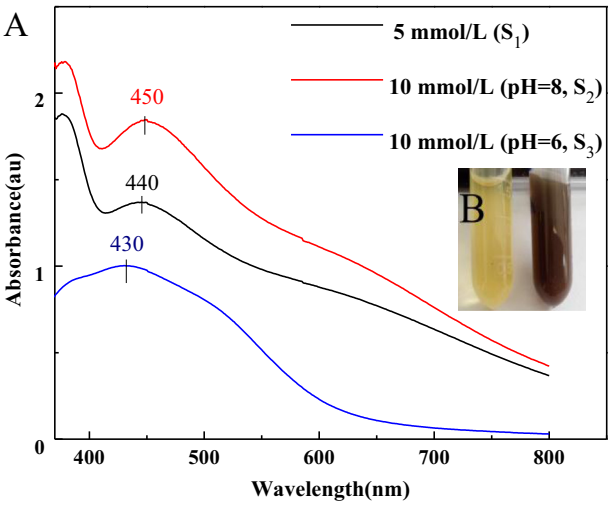

Fig. 1. UV–Vis absorption spectra of $Ag/Ag^{+}/Ag^{3+}$ synthesized by pomegranate rind extract (A). Color change of the mixture during reaction (B). (For interpretation of the references to colour in this figure legend, the reader is referred to the web version of this article.)

Research shows that when the nanoparticles are spherical or nearly spherical, the absorption peak of UV–Vis appears only with a single SPR resonance, whereas anisotropic particles will show two or three SPR resonances in accordance with their shapes [19]. In this work, the synthesized AgNPs by pomegranate peel extract were spherical or nearly spherical.

Note: In the silver nanoparticles, there exist actually substances of Ag, Ag_2O and AgO. In Ag_2O, Ag^+ exists. According to the silver valence electron structure and ionization potential, Ag^{2+} does not exist in AgO, while the most possible form is Ag_2O_2, in which either Ag^+ or Ag^{3+} is present. Ag_2O_2 can be written in a salt form: Ag(I) [Ag(III)O_2]. In anion $[AgO_2]^-$, the silver is Ag^{3+}, while the cation is Ag^+. Thus, the composite should be written as Ag/Ag_2O/AgO according to its composition. However, to better reflect its strong oxidation property and simplify its representation, it can be written in $Ag/Ag^+/Ag^{3+}$.

Previous study showed that pomegranate peel contains polyphenols, vitamins, protein, esters, flavonoids, etc. Polyphenols, vitamin C and other substances contain hydroxyl group that is of strong reducibility. The hydroxyl group can reduce silver ions into silver. Biological macromolecules containing amino and carbonyl groups exhibited a strong complexation for silver and silver ions, which were wrapped on the surface of AgNPs to come into the effect of dispersion and protection.

From the viewpoint of chemical thermodynamics, the biological macromolecules in the extract coated AgNPs, which can reduce the free energy on the surface of the particles to avoid aggregating to grow up. The free energy (surface tension) on the surface of nanoparticles, especially those newly formed, is very high, so the nanoparticles are unstable and easily to agglomerate into larger particles to each other to make the surface energy decreased. This process is spontaneous. That is why nano materials are very easily aggregated to grow up.

During the process of preparation of AgNPs by the pomegranate peel extract, AgNPs were wrapped by biological macromolecules, reducing the surface free energy to protect the nanoparticles from aggregation. In addition, in the case of the same volume, the energy of the system can be reduced to the minimum during the formation of spherical particles rather than any other shapes because the spherical shape occupies the smallest surface area.

In order to confirm the UV–Vis results, TEM was adopted to characterize the morphology and size of $Ag/Ag^+/Ag^{3+}$ nanocomposites. As shown in Fig. 2A, the nanocomposites were spherical and nearly spherical grains. The size ranged between 15 and 35 nm. Fig. 2B–D shows high-resolution TEM images of the nanocomposites, from which it can be seen that obvious grain lattice fringes appeared in the single nanograin. The distance between the lattice fringes was 0.23 nm, which is very close to the surface distance (0.235 nm) of the pure AgNPs (JCPDS file No. 04-0783) [27]. This result showed that the prepared AgNPs were of high crystallinity.

Analysis by XRD and FTIR

In order to confirm the composition and crystallinity of the obtained nanopowder, XRD was used for further detection and analysis. As shown in Fig. 3, there existed five obvious and very narrow diffraction peaks at $2\theta = 38.118$, 44.304, 64.450, 77.407 and 81.550. They represented, respectively, diffraction peaks of five crystal faces of pure AgNPs at (111), (200), (220), (311), and (222) (JCPDS file No. 5-2872). In addition, other labeled diffraction peaks were, respectively, those of the crystal surface of AgO (Ag^{3+}) (JCPDS, file No. 84-1108) and Ag_2O (Ag^+) (JCPDS, file No. 42-0874). They might be covered on the surface of the AgNPs. The average size of the nanocomposites was calculated by Debye Scherrer's formula. The results were 19.5, 34.3 and 33.1 nm, respectively, which was in agreement with those tested by TEM.

FTIR method was applied to analyze the combination of biological molecules and composites in the synthesis of $Ag/Ag^+/Ag^{3+}$ nanocomposites to further confirm the reduction and dispersion of chemical components in pomegranate peel. The pomegranate peel extracts before and after the synthesis of $Ag/Ag^+/Ag^{3+}$ nanocomposites were detected by FTIR to draw two corresponding plots Fig. 4a and b as shown in Fig. 4. As can be seen from the figure, there was a strong absorption peak at 3370.99 cm^{-1} on Fig. 4a curve, which was caused by the N—H stretching vibration in the amide group. In Fig. 4b curve, this peak became weak, blue shifting to 3040.99 cm^{-1} which indicated that the N—H bond chelated with silver ions. The brand 2926 ± 5 cm^{-1} belonged to the range of antisymmetrical stretching vibration absorption of alkene double bonds. Compared to the absorption of 2928.61 cm^{-1} at Fig. 4a curve, the absorption at Fig. 4b curve was significantly weaker, which showed that the alkene double bond was oxidized in the reduction reaction, while silver ions were reduced [28].

1724.90 cm^{-1} at Fig. 4a curve was the C=O stretching vibration absorption of flavonoids and amides in the extraction liquid. Absorptions in 1350.46 and 1232.92 cm^{-1} were caused by C—N stretching vibration or —C—N stretching vibration of the aromatic amino groups. The absorption at 1724.90 cm^{-1} in Fig. 4b curve was decreased, indicating that, in the reaction solution, C=O bond was oxidized. The absorptions at 1350.46 and 1232.92 cm^{-1} were red shifted or disappeared, indicating that complex reactions took place between the C—N or —C—N and silver ions [29]. 1616.09 and 1060.33 cm^{-1} at Fig. 4a curve were from stretching vibration absorption peaks of C—OH of protein and polyphenol in the pomegranate peel extract and of C—H of alkene. At 1616.09 cm^{-1} on Fig. 4b curve, blue shift occurred to 1685.23 cm^{-1}, showing that a substitution reaction and an electron induced effect possibly took place. At 1060.33 cm^{-1}, red shift moved to 1045.92 cm^{-1}, indicating that C—OH in protein and polyphenol was oxidized. In addition, protein and other macromolecular substances can be chemically combined with Ag or Ag^+ and Ag^{3+} to be wrapped on the surface of nano-Ag or to be used to protect the oxidized Ag^{3+} in the solution [30]. FTIR analysis showed that in the synthesis process of $Ag/Ag^+/Ag^{3+}$ nanocomposites, amide group, amino, carbonyl group, and polyphenolic compounds in the pomegranate extract played roles of reduction, dispersion and protection.

Characterization of antibacterial properties of $Ag/Ag^+/Ag^{3+}$ nanocomposites

As shown in Fig. 5, the diameter of the antibacterial circle of the $Ag/Ag^+/Ag^{3+}$ nanocomposites reached almost 14 mm. The maximum diameters of the antibacterial circles against *E. coli* and *S. aureus* were 12.56 mm (Fig. 5A) and 11.32 mm (Fig. 5B), respectively. Compared with the diameters of the inhibition zone on the sterile filter papers Nos. 3 and 5, those on the Nos. 2 and 4 were obvious. This is because that Ag^+ and Ag^{3+} are of high charges and small radius compared to Ag. They have strong adsorption capacity, and are more easily combined with phosphatide on the surface of the cell, amino groups in protein, carbonyl group, negative oxygen ions, disulfide bond in DNA (a cell membrane consists of two layers of phospholipid inlaid with biological macromolecules such as proteins. DNA contains the —S—S— bond). Small radius makes it easy for Ag^+ and Ag^{3+} to penetrate the cell membrane to damage the cell. So, $Ag/Ag^+/Ag^{3+}$ nanocomposites had a strong inhibitory effect against gram negative and gram positive bacteria.

Formation mechanism of Ag^{3+} in the $Ag/Ag^+/Ag^{3+}$ nanocompsoites

In the synthesis of AgNPs, the raw materials were $AgNO_3$ and pomegranate extract. The synthesized AgNP composites contained Ag^+ and Ag^{3+}. During the process of AgNP composites, Ag^+ would be

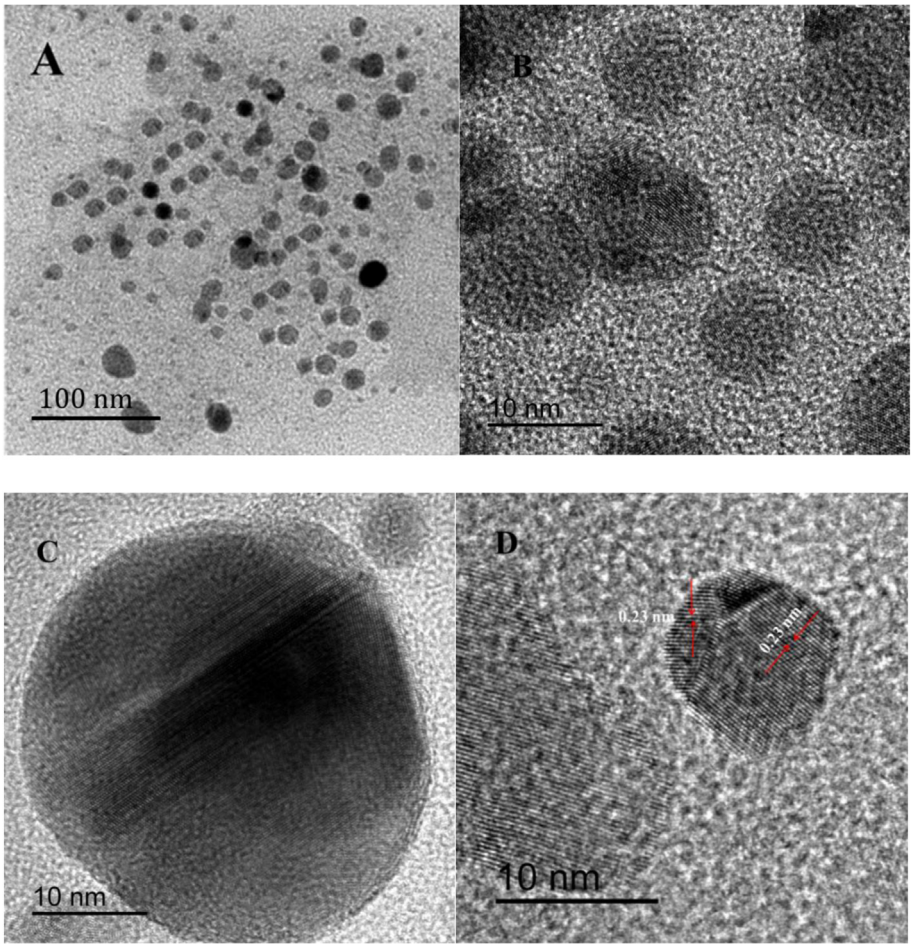

Fig. 2. TEM images of $Ag/Ag^{+}/Ag^{3+}$: (A)–(D) are the high-resolution images of a single nanocrystal showing lattice fringes with spacing of 0.23 nm.

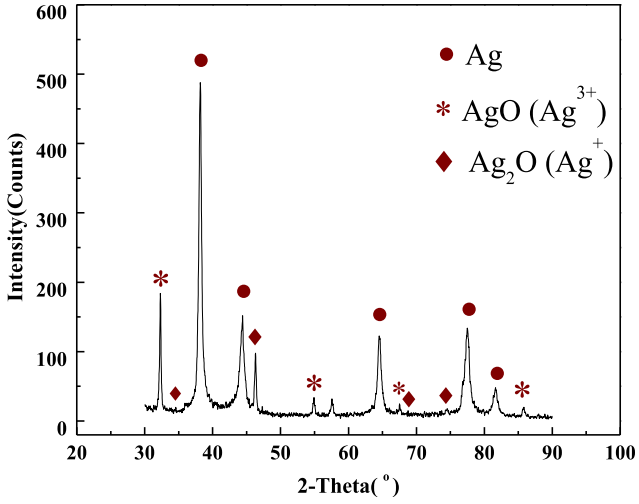

Fig. 3. XRD pattern of dried $Ag/Ag^{+}/Ag^{3+}$ nanoparticle powder.

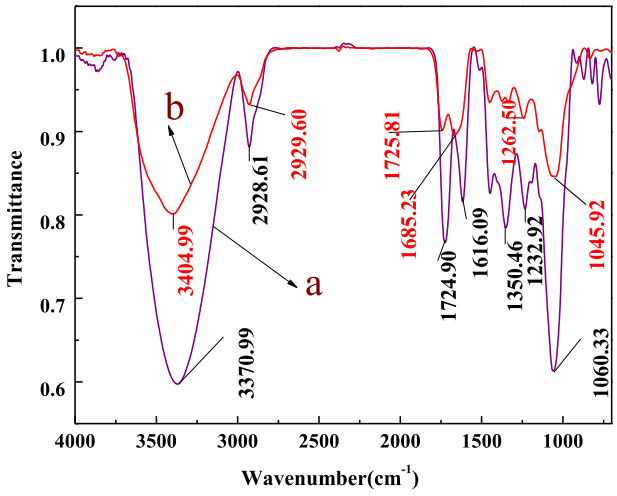

Fig. 4. Comparison of FTIR spectra of original granatum extract (a) and pomegranate rind extract (b) after synthesis of $Ag/Ag^{+}/Ag^{3+}$ nanoparticles.

wrapped into AgNPs. This is why Ag^{+} existed in the prepared nanocomposites. In the synthetic system of AgNPs, the silver ion existed in a complex formation or it was adsorbed on the surface of biological macromolecules. The Ag^{+} complex was entrained into the nanoparticles prior to reduction before AgNPs was wrapped. The presence of Ag^{3+} was related to two processes: the first was that Ag^{+} was oxidized to Ag^{3+} and the second was that Ag^{3+} was protected to exist in the nanoparticles. The oxidation of Ag^{3+} is very strong. It can hardly exist in the solution or Ag^{+} was oxidized to Ag^{3+}. From the perspective viewpoint of chemical thermodynamics, the ionic potential of Ag^{3+} is great and it has a strong complexation, so Ag^{3+} existed in a form of complex ions in the synthesis system, and the Ag^{3+} complex was very stable, leading to the very small concentration of free Ag^{3+} in the solution. According to the

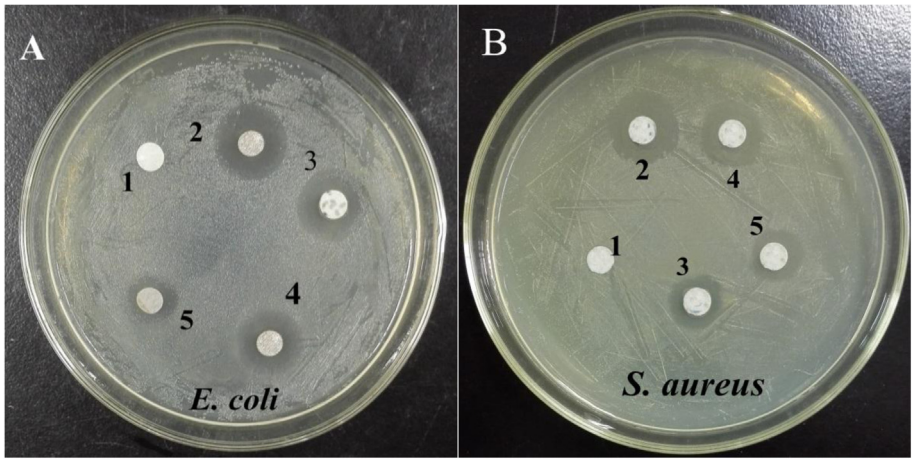

Fig. 5. Antibacterial activities of $Ag/Ag^{+}/Ag^{3+}$ nanoparticles against (A) *E. coli*, and (B) *S. aureus*. Sterile Whatman paper disks ($D = 5$ mm) are denoted as No. 1–5: No. 1 is a blank sample, Nos. 2 and 4 contain 10 μL of the $Ag/Ag^{+}/Ag^{3+}$ nanoparticles (1.16×10^{-4}, 7.23×10^{-6} mol/L), Nos. 3 and 5 contain 10 μL of the same concentrations of $AgNO_3$ solution. After 24 h incubation at 37 °C, the diameter (mm) of the inhibition zone was measured.

calculation by the Nernst equation, the electrode potential $E_{(Ag^{3+}\text{ complex ion}/Ag^{+}\text{ complex ion})}$ or $E_{(Ag^{3+}\text{ complex ion}/Ag\text{ complex})}$ was very small, less than that of the synthetic system E (O_2/H_2O). Consequently, in the formation of AgNPs, especially at the later stage, O_2 (g) existing in the reaction system oxidized Ag^{+} into Ag^{3+} which went into the AgNPs. Due to the strong complexation, Ag^{3+} can exist in the complex form, the formation mechanism of the complex in detail needs further investigation.

Conclusions

Pomegranate peel extract was mixed with silver nitrate solution (10 mmol/L) at the ratio of 1:2 v/v and pH = 8 of the mixture solution to have obtained $Ag/Ag^{+}/Ag^{3+}$ nanocomposites of spherical shape and good crystallinity, the size of which ranged from 15 to 35 nm, which verified that the pomegranate peel extract can replace chemical reducing agents and dispersants to reduce Ag^{+} into Ag to form a stable AgNP dispersion system. This provided a new way for the biosynthesis of nano-metal composites by oxidative metal ions.

The antibacterial experimental results indicated that when the concentration of $Ag/Ag^{+}/Ag^{3+}$ nanocomposites was 1.16×10^{-4} mol/L, it had strong bacteriostatic action against gram positive and gram negative bacteria. From FTIR spectra it is found that biomolecules were responsible for capping and stabilization in $Ag/Ag^{+}/Ag^{3+}$ nanocomposites.

In the process of synthesis of $Ag/Ag^{+}/Ag^{3+}$ nanoparticles by pomegranate peel extract, the volume ratio of the extract solution to $AgNO_3$ solution, the concentration of $AgNO_3$ and pH of the mixture were the main factors that affected the formation and size of the nanocomposites. The composition of the biological macromolecular from the pomegranate extract is complex. The mechanism of dispersion and stabilization of biological macromolecular needs further study.

Acknowledgments

This work was financially supported by the National "973" Preliminary Program Foundation of China (grant No. 2014CB260411) and the Academic Leaders Team Fund (grant No. 2013XSD 19). The authors acknowledge the School of Food and Biological Engineering, Shaanxi University of Science & Technology for providing UV–Vis, XRD, FTIR and SEM apparatus for experiments during the study.

References

[1] Reuther R. The NanoSustain and NanoValid project-two new EU FP7 research initiatives to assess the unique physical–chemical and toxicological properties of engineered nanomaterials. J Biomed Nanotechnol 2011;7(1):8–10.
[2] Liu Z, Yan J, Miao Y-E, et al. Catalytic and antibacterial activities of green-synthesized silver nanoparticles on electrospun polystyrene nanofiber membranes using tea polyphenols. Compos B Eng 2015;79(2):17–23.
[3] Emmanuel R, Palanisamy S, Chen SM, et al. Antimicrobial efficacy of green synthesized drug blended silver nanoparticles against dental caries and periodontal disease causing microorganisms. Mater Sci Eng C 2015;56 (37):4–9.
[4] Marin S, Vlasceaun GM, Tiplea RE, et al. Applications and toxicity of silver nanoparticles: a recent review. Curr Top Med Chem 2015;15(16):1596–604.
[5] Abrigo M, Mcarthur SL, Kingshott P. Electrospun nanofibers as dressings for chronic wound care: advances, challenges, and future prospects. Macromol Biosci 2014;14(6):772–92.
[6] Wu J, Zheng YD, Wen XX, et al. Silver nanoparticle/bacterial cellulose gel membranes for antibacterial wound dressing: investigation in vitro and in vivo. Biomed Mater 2014;9(3):373–9.
[7] Chen X, Schluesener HJ. Nanosilver: a nanoproduct in medical application. Toxicol Lett 2008;176(1):1–12.
[8] Mannl U, Van Den Berg C, Magunje B, et al. Nanoparticle composites for printed electronics. Nanotechnology 2014;25(9):1–9.
[9] Boote BW, Byun H, Kim JH. Silver–gold bimetallic nanoparticles and their applications as optical materials. J Nanosci Nanotechnol 2014;14(2):1563–77.
[10] Zhang LB, Wang EK. Metal nanoclusters: new fluorescent probes for sensors and bioimaging. Nano Today 2014;9(1):132–57.
[11] Majdalawieh A, Kanan MC, El-Kadri O, et al. Recent advances in gold and silver nanoparticles: synthesis and applications. J Nanosci Nanotechnol 2014;14 (7):4757–80.
[12] Kheybari S, Samadi N, Hosseini SV, et al. Synthesis and antimicrobial effects of silver nanoparticles produced by chemical reduction method. Daru 2010;18 (3):168–72.
[13] Moulton MC, Braydich-Stolle LK, Nadagouda MN, et al. Synthesis, characterization and biocompatibility of "green" synthesized silver nanoparticles using tea polyphenols. Nanoscale 2010;2(5):763–70.
[14] Gholami-Shabani M, Akbarzadeh A, Norouzian D, et al. Antimicrobial activity and physical characterization of silver nanoparticles green synthesized using nitrate reductase from fusarium oxysporum. Appl Biochem Biotech 2014;172 (8):4084–98.
[15] Pandey S, Mewada A, Thakur M, et al. Biogenic gold nanoparticles as flotillas to fire berberine hydrochloride using folic acid as molecular road map. Mater Sci Eng C 2013;33(7):3716–22.
[16] Ponarulselvam S, Panneerselvan C, Murugan K, et al. Synthesis of silver nanoparticles using leaves of *Catharanthus roseus* Linn. G. Don and their antiplasmodial activities. Asian Pac J Trop Biomed 2012;2(7):574–80.
[17] Sadeghi B, Gholamhoseinpoon F. A study on the stability and green synthesis of silver nanoparticles using *Ziziphora tenuior* (Zt) extract at room temperature. Spectrochim Acta Part A Mol Biomol Spectrosc 2015;134 (3):310–5.
[18] Faghri Zonooz N, Salouti M. Extracellular biosynthesis of silver nanoparticles using cell filtrate of *Streptomyces* sp. ERI-3. Sci Iran 2011;18(6):1631–5.
[19] Mahdieh M, Zolanvari A, Azimee AS, et al. Green biosynthesis of silver nanoparticles by *Spirulina platensis*. Sci Iran 2012;19(3):926–9.
[20] Juibari MM, Abbasalizadeh S, Jouzani GS, et al. Intensified biosynthesis of silver nanoparticles using a native extremophilic *Ureibacillus thermosphaericus* strain. Mater Lett 2011;65(6):1014–7.

[21] Rajesh S, Dharaniahanthi V, Kanna AV. Antibacterial mechanism of biogenic silver nanoparticles of *Lactobacillus acidophilus*. J Exp Nanosci 2015;10 (15):1143–52.
[22] Sathiyanarayanan G, Kiran GS, Selvin J. Synthesis of silver nanoparticles by polysaccharide bioflocculant produced from marine *Bacillus subtilis* MSBN17. Colloid Surf B 2013;102:13–20.
[23] Girilal M, Fayaz AM, Balaji PM, et al. Augmentation of PCR efficiency using highly thermostable gold nanoparticles synthesized from a thermophilic bacterium, *Geobacillus stearothermophilus*. Colloid Surf B 2013;106(16):5–9.
[24] Parikh RY, Ramanathan R, Coloe PJ, et al. Genus-wide physicochemical evidence of extracellular crystalline silver nanoparticles biosynthesis by *Morganella* spp.. PLoS ONE 2011;6(6):1–7.
[25] Soni N, Prakash S. Microbial synthesis of spherical nanosilver and nanogold for mosquito control. Ann Microbiol 2014;64(3):1099–111.
[26] Ahmed MJ, Murtaza G, Mehmood A, et al. Green synthesis of silver nanoparticles using leaves extract of *Skimmia laureola*: characterization and antibacterial activity. Mater Lett 2015;153:10–3.
[27] Philip D. Rapid green synthesis of spherical gold nanoparticles using *Mangifera indica* leaf. Spectrochim Acta Part A Mol Biomol Spectrosc 2010;77(4):807–10.
[28] Ashokkumar S, Ravi S, Kathiravan V, et al. Synthesis, characterization and catalytic activity of silver nanoparticles using *Tribulus terrestris* leaf extract. Spectrochim Acta Part A Mol Biomol Spectrosc 2014;121:88–93.
[29] Philip D, Unni C, Aromal SA, et al. *Murraya koenigii* leaf-assisted rapid green synthesis of silver and gold nanoparticles. Spectrochim Acta Part A Mol Biomol Spectrosc 2011;78(2):899–904.
[30] Amooaghaie R, Saeri MR, Azizi M. Synthesis, characterization and biocompatibility of silver nanoparticles synthesized from *Nigella sativa* leaf extract in comparison with chemical silver nanoparticles. Ecotoxicol Environ Saf 2015;120:400–8.